Probabilistic Model for Sensor Fault Detection and Identification

Nasir Mehranbod and Masoud Soroush
Dept. of Chemical Engineering, Drexel University, Philadelphia, PA 19104

Michael Piovoso
Pennsylvania State University, School of Graduate Professional Studies, Malvern, PA 19355

Babatunde A. Ogunnaike
DuPont Central Science and Engineering, Experimental Station, E1/104,Wilmington, DE 19880

A new Bayesian belief network (BBN) model with discretized nodes is proposed for fault detection and identification in a single sensor. The single-sensor model is used as a building block to develop a BBN model for all sensors in the process considered. A new fault detection index, a fault identification index, and a threshold setting procedure for the multisensor model are introduced. The fault detection index exploits the probabilistic information of the multisensor model, which, along with the proposed threshold setting procedure, leads to effective detection of faulty sensors. The fault identification index uses only the probabilistic information of the faulty sensor to determine in a discretized fashion the size of faults that should be analyzed within a moving time window to identify the fault type. Single-sensor model design parameters (prior and conditional probability data) are optimized to achieve maximum effectiveness in detection and identification of sensor faults. The single-sensor model and optimal values of design parameters are used to develop a multisensor BBN model for a polymerization reactor at steady-state conditions. Its capabilities to detect and identify bias, drift, and noise in sensor readings are illustrated for single and simultaneous multiple faults by several case studies.

Introduction

To achieve effective control/monitoring of a process, regardless of its complexity, reliable measurements from the process sensors are needed. An instrument (sensor) often comprises of different parts such as a sensing device, transducer, signal processor, and communication interface. Any of these parts may malfunction causing the sensor to generate signals with unacceptable deviation from its normal condition. A sensor working under this condition (faulty sensor) may cause process performance degradation, process shutdown, or even fatal accidents. To determine the presence of faulty sensors in a process and the type of the faults (bias, drift, noise, or complete failure), a method of instrument fault detection and identification (IFDI) is needed. Processes like nuclear power plants and highly exothermic chemical reactors are safety-critical in nature, and IFDI is of vital importance to their safe and effective operation. The application of IFDI is not restricted to extreme cases such as nuclear power plants, and the benefits of IFDI implementation are well recognized in other fields (Lee et al., 1997). Because of stricter safety and environmental regulations, as well as increasingly competitive global market conditions, IFDI has in recent years received more attention.

Preventive maintenance and automated techniques are common methods of IFDI. Preventive maintenance is basi-

Correspondence concerning this article should be addressed to M. Soroush.

cally regular checking and calibration of sensors. Even the tedious procedure of preventive maintenance cannot guarantee a sensor fault-free system, and, hence, it cannot be considered as a perfect alternative for an automated and efficient IFDI system. The automated IFDI techniques that are based on either analytical or physical redundancy methods (Betta and Pietrosanto, 2000). Measuring (inferring) a parameter/variable by (from) more than one sensor is the basis of the physical redundancy methods (Park and Lee, 1993; Alag et al., 1995; Dorr et al., 1997). For the purpose of fault detection, only two measurements are enough. However, to extend this to fault isolation, three or more measurements are necessary. The physical redundancy methods are relatively easy to implement. They provide a high degree of certainty, although they suffer from the disadvantage of requiring additional sensors.

Kalman filters, Luenberger observers, parity relations, principal component analysis (PCA), and artificial neural networks are the analytical redundancy methods that have received a lot of attention. Kalman filters and Luenberger observers have been used widely for IFDI (Clark et al., 1975; Clark, 1978a,b; Frank and Keller, 1980; Patton and Chen, 1997). Apart from the inadequacies that may be caused by the linear approximation of process model used in EKF, one needs a set of "matched filters" (dedicated observers) for each sensor to perform fault isolation task (Mehra and Peshon, 1971; Watanabe and Himmelblau, 1982; Watanabe et al., 1994). The application of Kalman filters and Luenberger observers requires a process model. However, the existence of systematic methods of designing filters and observers is a major advantage.

PCA and parity relations are closely related (Gertler and McAvoy, 1997) and are applied for fault detection and diagnosis (Gertler and McAvoy, 1997; Gertler et al., 1999). PCA has proved to be an effective tool for monitoring of complex chemical processes (MacGregor, 1989; Kresta et al., 1991; Piovoso et al., 1992a,b; Wise et al., 1995) and has been successfully used for IFDI for processes operated at steady state (Qin and Li, 1999). The main feature of PCA, its capability of reducing the dimensionality of the process model, has made it an attractive and currently active research field (Valle et al., 2000; Yoon and MacGregor, 2000). Artificial neural networks have been used for gross error detection (Sanchez et al., 1996; Aldrich and Van Deventer, 1994; Terry and Himmelblau, 1993; Gupta and Shankar, 1993; Kramer, 1992) and in combination with a state observer as an isolation tool for faulty sensors (Bulsari et al., 1991).

There have been a few attempts to apply Bayesian belief networks for fault detection and diagnosis. Kirch and Kroschel (1994) proposed an approach to present a BBN model in the form of a set of nonlinear equations and constraints that should be solved for the unknown probabilities. As an inference tool, Rojas-Guzman and Kramer (1993) used the genetic algorithm in BBN for fault diagnosis. Santoso et al. (1999) exploited the learning capability of Bayesian belief networks to use process data in an adaptable fault diagnosis strategy. Bayesian belief networks have also been applied for IFDI. While Nicholson and Brady (1992) and Ibarguengoytia et al. (1996) focused on detection of faulty sensors, Aradhye (1997) explored the use of Bayesian belief networks for both detection and identification of sensor faults. However, he considered an ideal case of no practical importance and did not address the effect of design parameters of his BBN model (prior and conditional probability data) on IFDI performance and the issue of threshold setting for discretized nodes.

In this article, we propose a single-sensor BBN model, which is a result of studying the IFDI performance of several model structures. The single-sensor model is used as a building block to develop a BNN model for all sensors in the process under consideration. A new fault detection index, a fault identification index, and a threshold setting procedure for the multisensor model are introduced. The fault detection index exploits the probabilistic information of the multisensor model, which along with the proposed threshold setting procedure leads to effective detection of faulty sensors. The fault identification index only uses the probabilistic information of the faulty sensor to determine in a discretized fashion the size of faults that should be analyzed within a moving time window to identify fault types. Single-sensor model design parameters (prior probability data, number of states for each node, and node bin-size assignments) are optimized to achieve maximum effectiveness in detection and identification of sensor faults. The single-sensor model and the optimal values of the design parameters are used to develop a multisensor BBN model for a polymerization reactor at steady-state conditions. The capabilities of this BBN model to detect and identify bias, drift, and noise in sensor readings are illustrated in the cases of single and simultaneous multiple faults.

A brief review is presented of the theory of BBN and the features of the existing single-sensor BBN models. A new model and indices for detection and identification of sensor faults are presented. The effect of design parameters of the new model on its IFDI performance, the optimal values of the design parameters, and the issue of threshold setting are also discussed. Finally, the application and performance of the IFDI method are shown by considering a polymerization reactor.

Bayesian Belief Networks: A Review

BBN theory

A BBN consists of a set of variables and a set of directed edges between them. The nodes in the network represent prepositional variables. Each variable has a finite set of mutually exclusive states (discretized into finite states). It is also possible to have a combination of continuous and discretized variables in a BBN (Lauritzen and Spieglhalter, 1988). The directed link between two nodes represents a causal influence of one node (parent node) on the other (child node). The combined set of variables and directed edges form a directed acyclic graph. Associated with each child node is a probability distribution (Conditional Probability, CP) that is dependent on the probability distribution of its parents. The nodes with no parents are called "root nodes" and the probability distribution of these nodes is called prior probability (PP). The directed structure of the network, and the conditional and prior probability distributions represent our knowledge of the system.

A BBN can be represented as

$$BBN = [V, L, PP, CP] \tag{1}$$

where V is the set of variables or nodes and L is the set of directed links. The external information on any node at any instant is referred to as evidence and is presented to the network by instantiating the probability distribution of the corresponding node. Our knowledge of the system and the evidences allow calculation of new probability distributions of the uninstantiated nodes in the network (belief updating). The process of belief updating in the light of the evidences introduced to the BBN is called "inference" (evidence propagation). Bayes' rule is the basis for probabilistic inference processes

$$P(A|E) = \frac{P(E|A)P(A)}{P(E)} \tag{2}$$

where E (evidence) and A are prepositional variables, $P(i)$ and $P(i|j)$ are the probability distribution of the prepositional variable "i" and probability distribution of "i" given probability distribution of the prepositional variable "j". In the context of IFDI, the evidences are the sensor readings and the updated beliefs should be used for detection and identification of emerging sensor faults. The application of Bayesian belief networks for IFDI has been explored to some extent, and the next subsection provides a review of the previous research in this field.

Existing single-sensor BBN models

The probabilistic nature of BBN provides a powerful framework that can be used for IFDI. However, its capabilities and limitations for IFDI have been explored to a limited extent. The existing work in this field includes the studies by (a) Nicholson and Brady (1992) and Ibarguengoytia et al. (1996), who focused only on detection of faulty sensors, and (b) Aradhye (1997), who concentrated on both detection and identification of sensor faults. Basically, there are two existing BBN models to represent a single sensor: one was proposed by Rojas-Guzman and Kramer (1993) and the other by Aradhye (1997).

Ideally, an IFDI method should be capable of performing the two major tasks of detection and identification of sensor faults in one step. In particular, it should be able to carry out the following *ideal* tasks:

- T1. Fault detection in the sensor once a fault occurs.
- T2. Identification of the fault type and its magnitude after the detection task (T1) has been completed.
- T3. Tasks T1 and T2 in one step (IFDI require analysis of sensor readings in one snapshot).

Throughout this article, the suitability of several single-sensor models for IFDI is evaluated in terms of these ideal tasks.

Model I

Rojas-Guzman and Kramer (1993) studied BBN as a tool for fault diagnosis of chemical processes. They proposed the model depicted in Figure 1, which is referred to as Model I. Here, X_a is a node representing the actual value of the parameter/variable "a" that is measured, B_a is a node representing bias associated with X_a, N_a is a node denoting noise associated with X_a, and R_a is a node representing the available measurement for X_a. Rojas-Guzman and Kramer (1993) used Model I just as an example to demonstrate the application of Monte Carlo simulation for generating the conditional probability data. IFDI was not their objective, and, therefore, they did not attempt to study the IFDI performance of Model I.

In Model I, because the measurement (R_a) is affected by both bias (B_a) and noise (N_a), performing IFDI requires analyzing the updated probabilities of the B_a and N_a nodes. Deviation of state probabilities of the B_a and N_a nodes from their normal values (that is the values that the probabilities take when there is no fault) is indicative of a fault. A method to quantify such deviations and a proper threshold-setting procedure allow one to perform task T1. Task T2 necessitates (i) differentiating between bias and noise as fault type and (ii) distinguishing between states of the B_a and N_a nodes to determine fault magnitude. In real life problems, different types of faults (causes) can create the same sensor reading (effect) in one snapshot. In other words, one-to-one mapping of causes and effects does not exist in practical problems. Therefore, analyzing the updated probabilities of nodes B_a and N_a in one snapshot or over a period of time cannot be used to determine the fault type. This implies that task T3 (tasks T1 and T2 in one step) cannot be carried out by using Model I.

Model II

The work of Aradhye (1997) is the first attempt to use BBN for IFDI. He proposed the model shown in Figure 2, which is referred to as Model II. Unlike Model I with four nodes, Model II has three nodes. In Model II, nodes X_a and R_a are the same as in Model I, and node S_a represents the status of the sensor. Both Models I and II are based on the fact that bias (B_a) and noise (N_a) affect the sensor reading (R_a). The only difference between these two models is that the two

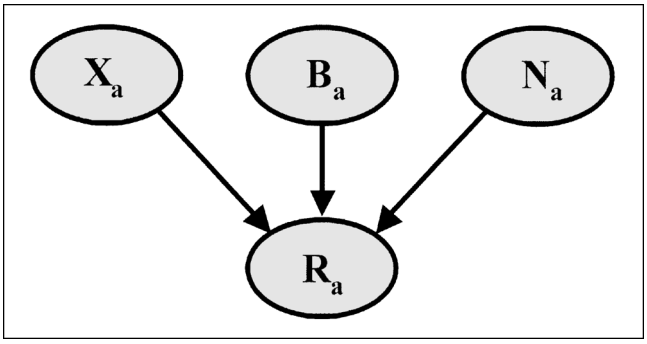

Figure 1. BBN Model I.

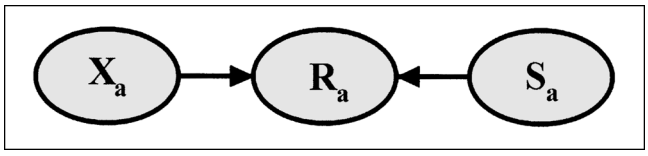

Figure 2. BBN Model II

nodes B_a and N_a of Model I are clustered into the node S_a in Model II. When the actual value of the variable, X_a is normal, a deviation of the measurement (R_a) from its normal value is due to a change in the state probability of node S_a. Therefore, the updated probabilities of node S_a should be analyzed for both detection and identification of sensor faults.

Aradhye (1997) suggested the following number of states for node S_a, depending on the purpose of the network: (i) two states (operative, faulty) for fault detection, and (ii) more than two states for IFDI (each of the states represent one of the possible operating conditions of a sensor). To perform IFDI, he used four states for node S_a in his work to represent four different operating conditions of a sensor that are normal, bias, noise, and complete failure. These states are functions that act upon the probability distribution of node X_a to generate the corresponding probability distribution for node R_a. While fault detection (task T1) is performed through observing the probability of the state denoting normal operation, fault identification (task T2) is achieved by analyzing the updated probabilities of the other three states of node S_a. Aradhye (1997) chose the fault functions (bias, noise, and complete failure) of node S_a such that each function modifies the probability distribution of node X_a in a specific and distinguishable way, which does not correspond to any practical situation. His unrealistic fault functions describe one-to-one mapping between causes and effects, allowing Model II to do task T3. Since the one-to-one mapping does not exist in practice, Model II has no practical use. Furthermore, the work did not address the important issue of threshold setting.

Single-Sensor BBN Model III

The analysis of IFDI performance of Models I and II indicated the inadequacy of the models for IFDI. Motivated by this, we propose a new model that cannot perform task T3, but is powerful enough to achieve effective IFDI. An IFDI method is developed on the basis of the new model and is then presented. Application of the IFDI method requires the following assumptions to hold:

- **No process, controller, or actuator faults.** There should be no shift in process operating conditions due to changes in characteristic parameters of the process, unmeasured disturbances, controller failure, or actuator failure.
- **Availability of frequent measurements.** All sensors included in a BBN provide frequent measurements.
- **IFDI execution period greater than or equal to the measurement sampling period.** The IFDI execution period is assumed to be equal or greater than the sampling period of the sensor measurements.
- **Availability of process model or process data.** A sufficiently accurate process model or fault-free process data (from normal operation) is available to describe the correlations among the process variables.
- **No simultaneous fault types in one sensor.** Faults of different types [drift, bias and noise (white noise)] do not occur simultaneously in one sensor.

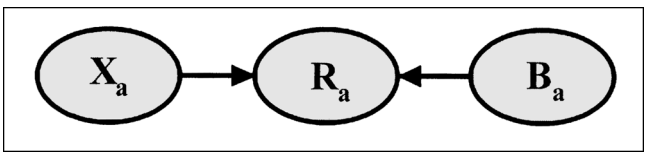

Figure 3. BBN Model III.

Structure of Models III

Model III, shown in Figure 3, consists of the three discretized nodes X_a, R_a, and B_a, that are related by the mathematical model

$$\text{Sensor reading } (R_a) = \text{Actual value}(X_a) + \text{Bias}(B_a) \quad (3)$$

Nodes X_a, B_a, and R_a, of Model III have the same definitions as those of Model I with mutually exclusive states. To develop a multisensor BBN model for sensors in a process, one needs to connect the single-sensor BBNs (models) developed using Model III to each other through the X_a nodes considering the cause-effect relation and the correlation between the X_a nodes. Node B_a in Model III plays a key role in performing IFDI, because both detection and identification of sensor faults by using Model III require analysis of the updated state probabilities of node B_a. While analysis of a snapshot data on updated state probabilities of node B_a is adequate for fault detection (task T1), fault identification (task T2) requires analysis of the updated state probabilities of node B_a over a sufficiently long period of time.

Fault Detection

Deviation of state probabilities of node B_a from their normal values (the values that the probabilities take when there is no fault) is indicative of a fault. Fault detection requires a method to quantify the deviation. To carry out this systematically, the following two definitions are introduced:

Definition 1: Probability absolute difference (PAD_{ij}) is defined as the difference between the updated probability of state j of node B_a of sensor i, $P(B_a)_{ij}$, and the probability of state j of node B_a of sensor i in operative mode, $P^*(B_a)_{ij}$, both expressed in terms of percentage

$$PAD_{ij} = \left| P(B_a)_{ij} - P^*(B_a)_{ij} \right| \qquad i = 1, \ldots, n,\ j = 1, \ldots, m \quad (4)$$

Definition 2: Sum of probability absolute differences for sensor i, S_{PAD_i}, is

$$S_{\text{PAD}_i} = \sum_{j=1}^{m} \text{PAD}_{ij} \qquad i = 1, \ldots, n \quad (5)$$

where n is the number of sensors in a multisensor BBN and m is the number of states of node B_a.

For a single-sensor BBN, where $n = 1$, the deviation of the sum of absolute differences from zero is indicative of a fault. However, for a multisensor BBN when faults emerge, because of the correlations among X_a nodes of sensors, the sum of absolute differences takes a value other than zero even for operative sensors. To determine the relative status of a

sensor with respect to other sensors in a multisensor BBN, the following fault detection index for sensor i is introduced:

Definition 3: Fault detection index for sensor i, D_i is defined as

$$D_i = 100 \frac{S_{\mathrm{PAD}_i}}{\sum_{i=1}^{n} S_{\mathrm{PAD}_i}} \quad i = 1, \ldots, n \tag{6}$$

This normalized index is basically a percentage of the sum of the sum-of-probability-absolute-differences. The index should be used in multisensor IFDI, where $n > 1$. Normalized indices have also been used for fault detection elsewhere. For example, Qin and Li (1999) defined a normalized index, which is sensitive to sensor faults that cause variance change. Normalization has also been used in calculating sensor validity index to measure sensor performance (Dunia et al., 1996).

To achieve effective fault detection (no false alarm or missed faults), the fault detection index of every sensor in a multisensor BBN should be evaluated using a proper threshold-setting procedure. The threshold setting procedure is proposed in the next subsection.

Threshold setting

Univariate or multivariate statistical methods are often used to determine thresholds for fault detection. While univariate statistical methods lack the benefit of using the correlations between process variables, the multivariate based methods like T^2 statistics incorporate such correlations in threshold setting, which results in reducing the rate of false alarms and missed faults. Neither of these two threshold-setting methods is applicable to the fault detection index proposed in this work. Because of the discrete mode of the nodes of Model III, the updated probabilities of B_a nodes and also the sum of probability absolute differences do not change as long as the sensor readings remain within the range of one state of node R_a. Therefore, the discrete mode of the nodes of Model III changes the nature of the sensor readings to the extent that the conventional threshold-setting procedures are not suitable for fault detection by using Model III. To explain this further, consider a sample of continuous sensor readings that represent normal operation with a mean of zero (dimensionless basis) and a variance of σ. Furthermore, assume that the bin range of the state of node R_a representing normal operation (N) is set such that it covers the span of σ. For the selected bin-range assignment of state N, the updated probabilities of node B_a and, thus, the sum of probability absolute differences do not change, because the evidence (state of node R_a) remains unchanged (regardless of the value of the sensor reading). To propose a threshold-setting procedure for fault detection by using Model III, half number $n_{1/2}$ is introduced by the following definition.

Definition 4: The half number ($n_{1/2}$) is defined as

$$\begin{cases} n_{1/2} = n/2 & (n \text{ is even}) \\ n_{1/2} = (n-1)/2 & (n \text{ is odd}) \end{cases} \tag{7}$$

The outcome of reasoning by using BBN for sensor fault detection depends on the number, coherency of evidences (sensor readings), and correlation among the sensor readings. As an example, analysis of the updated probabilities for fault detection often points to the group of faulty or operative sensors with a number of members exceeding the half number ($n_{1/2}$), as the operative group. Therefore, fault detection in cases in which the number of simultaneously-faulty sensors (l) exceeds the half number ($n_{1/2}$) may result in false alarms or missed faults. However, by employing a proper threshold-setting procedure, effective fault detection *is* feasible in cases that the number of simultaneously-faulty sensors is less than or equal to the half number ($l \le n_{1/2}$). To perform effective fault detection (no false alarms or missed faults), the fault detection threshold (T_d) should be set such that

$$Do_{\max} < T_d < Df_{\min} \tag{8}$$

where $Do_{\max}$ is the threshold lower bound, the maximum value that the fault detection index D_i takes for operative sensors. $Df_{\min}$ is the threshold upper bound, the minimum value that the fault detection index D_i takes for faulty sensors. For the ith sensor in a multisensor BBN, fault detection is then performed by the simple rule

$$\begin{cases} D_i > T_d & (\text{faulty sensor}) \\ D_i < T_d & (\text{operative sensor}) \end{cases} \tag{9}$$

False alarms happen when $T_d < Do_{\max}$, and missed faults occur when $T_d < Df_{\min}$. The reliability of the threshold lower and upper bounds depends on the level of uncertainty in the conditional probability data (that represents correlations among X_a nodes of a multisensor BBN). False alarms and missed faults can occur, if conditional probability data used in a multisensor BBN does not describe accurately correlations among X_a nodes. It is worth noting that the lower the difference is between threshold lower and upper bounds, the higher is the probability of false alarms and missed faults. As the number of simultaneously-faulty sensors approaches the half number, the weight assigned to measurements of faulty sensors increases, and, thus, the difference between threshold lower and upper bounds decreases to a minimum when $l = n_{1/2}$. Cases in which $l = n_{1/2}$ represent the hardest, but achievable, fault detection task that one could attempt by using BBN. A fault detection threshold, leading to effective fault detection in these difficult cases, ensures the reliability of fault detection for less difficult cases with $l \le n_{1/2}$.

A method of threshold setting can be proposed on the basis of the half number. For a single-sensor BBN with node R_a consisting of m states, the number of possible faulty modes is m-1 (the one state not included represents normal operation). For a multisensor BBN developed by connecting n of such single-sensor BBNs, the number of possible faulty modes is $\{[n!\ (m-1)^{n1/2}]/[n_{1/2}!(n-n_{1/2})!]\}$ when $l = n_{1/2}$. To find a fault detection threshold that allows effective fault detection (no false alarms or missed faults), we propose using the data generated for D_i by simulating faulty modes for which $l = n_{1/2}$

to determine the values of threshold lower and upper bounds. The fault detection threshold should then be determined using Eq. 8. The closer is the value of fault detection threshold to $Df_{\min}$ or $Do_{\max}$, the higher is the probability for missed faults or false alarms. The task of threshold setting is basically a compromise between false alarms and missed faults. Such compromise should be done considering the tolerance of a process to false alarms or missed faults.

Fault identification

After fault detection in an IFDI procedure, fault identification can be carried out for faulty sensors. As mentioned earlier, fault identification using Model III requires analysis of the updated state probabilities of node B_a over a sufficiently long period of time. Such analysis can be carried out by using the most probable state (MPS) and the fault identification index that are defined below.

Definition 5: The most probable state is the state of node B_a that is most probably responsible for the detected fault.

Definition 6: Fault identification index for faulty sensor i, I_i, is defined as

$$I_i = \max_j \left(\mathrm{PAD}_{ij}\right) \; j = 1, \ldots, m \text{ and } j \neq k \qquad (10)$$

where state k is the state representing normal operation.

The first step in fault identification is to use the updated probabilities of node B_a in a snapshot to determine the most probable state. The state of node B_a with a probability absolute difference equal to the fault identification index is the most probable state. Tracking the status of the most probable state over a sufficiently long period of time is the second step that should lead to fault identification. A time-invariant MPS status over a sufficiently long period of time, a steady gradual change of MPS towards the higher or lower states of bias, and a steady fluctuation of MPS between different states of bias are indications of bias, drift, and noise (assumed to be white noise), respectively. As an example, consider node B_a with these five states: very negative ($n2$), negative ($n1$), zero (z), positive ($p1$), and very positive ($p2$), where the state z represents normal operation. Figure 4 depicts how the fault type (bias, drift and noise) can be identified for such a node B_a by using Model III. Measurement signals shown in these figures by solid lines are filtered sensor readings. The circles represent the status of the most probable state (MPS) that changes when the sensor reading crosses the bin-range of the states. The first section of Figure 4, sampling instance 0 to 55, shows two cases of bias in sensor reading. Each case starts with a rapid change followed by biased readings. The rapid changes are from state z to $p2$ and then from state $p2$ to $n2$, and the biased readings are within the bin-range of the states $p2$ and $n2$. The time-invariance of the MPS status over a relatively long period of time in the first section of Figure 4 indicates bias. The sensor reading in the second section of Figure 4, sampling instance 56 to 130, shows a steady gradual increase from state z to $p2$. Such changes in sensor reading, gradual changes towards the higher or lower states of the MPS status, are indicative of a drift. The third section of Figure 4, sampling instance 131 to 150, depicts the way that noise can be identified. The steady fluctuation of the MPS status between different states of bias indicates noise.

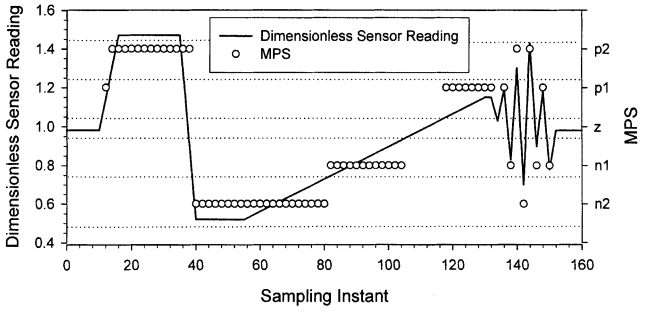

Figure 4. Identification of bias, drift, and noise by using Model III.

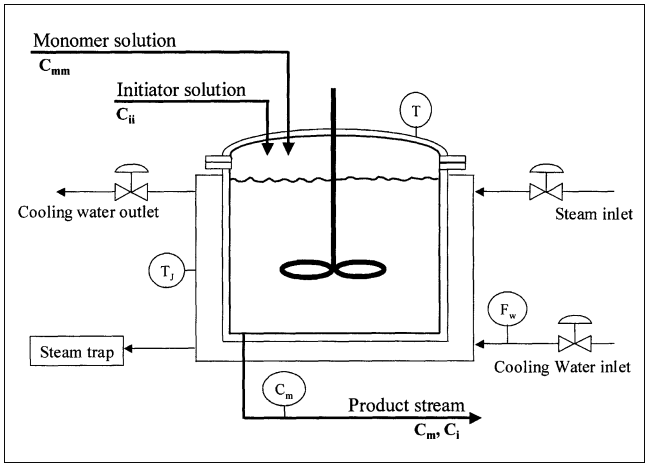

Figure 5. Polymerization reactor.

Case study: IFDI using Model III

To illustrate the application of the fault detection and identification procedures, a case study is presented in this subsection. Consider a continuous-stirred-tank reactor in which free-radical, solution polymerization of styrene takes place. The reactor is depicted in Figure 5. The steady-state version of the model in (Hidalgo and Brosilow, 1990) is used for calculating the conditional probabilities needed to build a multisensor BBN model for the process sensors. Here, F_w, T, T_J, C_{ii}, C_{mm}, and C_m represent the cooling water flow rate, reactor temperature, jacket temperature, concentration of initiator in the initiator stream, concentration of monomer in the monomer stream, and concentration of monomer in the outlet stream, respectively. F_w, T, T_J, and C_m are measured, and C_{ii} and C_{mm} are constant. Among the measured variables, only F_w can be adjusted arbitrarily. For the polymerization reactor, the subscript a in X_a, R_a, and B_a takes F_w, T, T_J and C_m.

To develop single-sensor BBN for each of the four measured variables ($n = 4$), the following five states ($m = 5$) are considered:

- very low (L2), low (L1), normal (N), high (H1) and very high (H2), for nodes X_a and R_a.

Table 1. Bin-Range Assignment for Nodes X_a, R_a and B_a

Node	Factor	States of Nodes X_a and R_a										
		$L2$		$L1$		N			$H1$		$H2$	
		ll*	ul*	ll	ul	ll	Steady State Value	ul	ll	ul	ll	ul
X_{F_w}	10^{-3}	[6.010	6.277)	[6.277	6.544)	[6.544	6.6773 m^3/s	6.811]	(6.811	7.078]	(7.078	7.345]
X_T	10^2	[4.750	4.675)	[4.675	4.610)	[4.610	4.590 (K)	4.581]	(4.581	4.526]	(4.526	4.476]
X_{T_j}	10^2	[4.698	4.582)	[4.582	4.479)	[4.479	4.447 (K)	4.432]	(4.432	4.346]	(4.346	4.269]
X_{Cm}	10^{-2}	[18.56	20.45)	[20.45	22.33)	[22.33	22.96 ($kmol/m^3$)	23.27]	(23.27	25.17]	(25.17	26.98]
		State of Node B_a										
		$n2$		$n1$		z			$p1$		$p2$	
		ll*	ul*	ll	ul	ll		ul	ll	ul	ll	ul
B_{Fw}	10^{-3}	[−0.65	−0.39)	[−0.39	−0.13)	[−0.13		0.13]	(0.13	0.39]	(0.39	0.65]
B_T	1	[−8.00	−4.80)	[−4.80	−1.60)	[−1.60		1.60]	(1.60	4.80]	(4.80	8.00]
B_{Tj}	1	[−12.85	−7.71)	[−7.71	−2.57)	[−2.57		2.57]	(2.57	7.71]	(7.71	12.85]
B_{Cm}	10^{-3}	[−25.85	−15.51)	[−15.51	−5.17)	[−5.17		5.17]	(5.17	15.51]	(15.51	25.85]

*ll = lower limit; ul = upper limit.

• very negative ($n2$), negative ($n1$), zero (z), positive ($p1$), very positive ($p2$), for node B_a.Table 1 presents the bin-range assignment for nodes X_a, R_a, and B_a. The bin size of the states of node B_a of each sensor is assigned as 1.1 times of the bin size of state N of the corresponding sensor. In Model III, X_a and B_a are parent nodes, and R_a is a child node. Table 2 lists prior probability distributions for the parent nodes. The conditional probability distributions for R_a nodes (not presented here) are generated by Monte Carlo simulation using the node bin-range assignments. The multisensor BBN model, shown in Figure 6, is developed for the polymerization reactor by connecting the single-sensor networks for the four process sensors through nodes X_{Fw}, X_T, X_{TJ}, and X_{Cm}. The probability distributions of nodes X_T, X_{TJ}, and X_{Cm} conditioned on X_{Fw} (conditional probability data) are calculated by the steady state version of the reactor mathematical model. The calculated conditional probability data are assumed to describe correlations among X_a nodes accurately.

Table 3 lists the probability distributions of B_a nodes for the developed multisensor BBN when all measurements (R_a) are within the range of state N. Netica API function library (Norsys Software Corp.) was used for all belief-updating calculations throughout this article. Table 4 presents the updated probability distributions of B_a nodes, calculated values of the probability absolute difference ($PAD_{i,j}$), the sum of probability absolute differences (S_{PADi}), and the fault detection index (D_i) in a snapshot for two cases:

(i) Case 1: a fault in R_{Fw} within the range of state L2

(ii) Case 2: faults in R_{Fw} and R_T within the ranges of states L1 and H1, respectively.

The values of the threshold lower and upper bounds (Do_{max} and Df_{min}) are determined to be 21.4 and 15.8, respectively. Since $Do_{max} > Df_{min}$, threshold setting according to Eq. 6 and successful fault detection for all cases with $1 \le l \le 2$ ($n_{1/2} = 2$) are not possible. For this case study, there is no preference between missed faults and false alarms, and, thus, the average of 21.4 and 15.8 (18.6) is considered as the value of the fault detection threshold (T_d). In Cases 1 and 2, fault detection is feasible with 18.6 as the fault detection threshold. The highlighted data among PAD_{ij} data of Table 4 are the fault identification index for faulty sensors. The fault identification index for Case 1 is $C_{Fw} = 99.784$ and for Case 2 is $C_{Fw} = 21.456$ and $C_T = 19.998$. In both cases, it distinguishes the MPS in one snapshot. Fault identification requires tracking the status of MPS over a sufficiently long period of time that is not included in this case study.

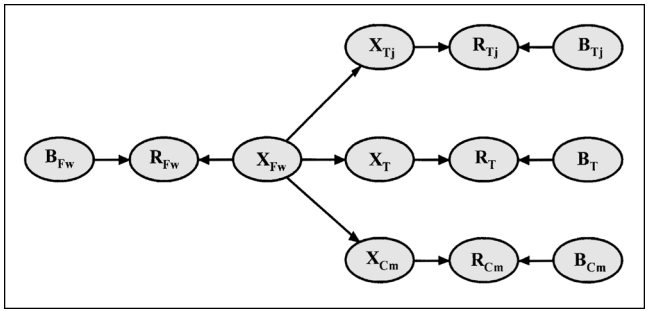

Figure 6. BBN of the polymerization reactor.

It was assumed in the previous paragraph that the conditional probability data of nodes X_T, X_{TJ}, and X_{Cm} represent the correlations between these nodes and node X_{Fw} accurately. Therefore, the arbitrarily chosen bin-range assignments and the prior probability distributions for this case study is the reason for Do_{max} to be greater than Df_{min}. The

Table 2. Prior Probability Data for Nodes X_a and B_a

Nodes	State Probabilities (out of 100)				
X_a	$P(L2) = 1.00$	$P(L1) = 4.00$	$P(N) = 90.00$	$P(H1) = 4.00$	$P(H2) = 1.00$
B_a	$P(n2) = 1.00$	$P(n1) = 4.00$	$P(z) = 90.00$	$P(p1) = 4.00$	$P(p2) = 1.00$

Table 3. State Probabilities for Nodes B_a (out of 100)

		j				
		1	2	3	4	5
i		$n2$	n1	z	$p1$	$p2$
1	F_w	0.002	1.691	96.541	1.758	0.006
2	T	0.004	1.616	94.559	3.622	0.200
3	T_j	0.004	1.609	94.422	3.752	0.213
4	C_m	0.014	1.801	96.428	1.751	0.006

fact that the design parameters affect the IFDI performance of Model III necessitates study of the effect of the design parameters on IFDI performance of Model III.

Optimum values of design parameters

This subsection provides detailed information on the optimum values of design parameters that maximize the effectiveness of the IFDI performance of Model III. To achieve the best IFDI performance for a single-sensor BBN, a criterion is introduced in the next subsection. The search constraints for the optimum values of design parameters are discussed in subsequent subsections, which also present the optimum values of design parameters.

IFDI Performance Index for a Single Sensor. To compare the effects of design parameters of a single-sensor BBN on the IFDI performance of the BBN, one needs a suitable index to quantify the performance. Since, for a single-sensor BBN, any value of the fault detection index (D) other than zero is an indication of a fault, the index should be only a measure of fault identification performance. In other words, fault detection for a single-sensor BBN can be performed effectively regardless of the values of design parameters without a need for the fault detection threshold setting. We propose using the following IFDI performance index (PI)

$$PI = \min_{i,j}\left(PD_{ij}\right) \begin{cases} i = 1,\ldots,m \text{ and } i \neq k \\ j = 1,\ldots,m,\ j \neq i \text{ and } j \neq k \end{cases} \quad (11)$$

Table 5. Single-Sensor Probability Difference for Two Different Sets of Design Parameters

		Design Parameter Set 1*				Design Parameter Set 2**			
		1	2	4	5	1	2	4	5
i	j	L2	L1	H1	H2	L2	L1	H1	H2
1	L2		0.48	27.4	27.57		8.56	31.18	31.37
2	L1	17.13		17.55	17.83	16.22		16.82	17.13
4	H1	18.02	17.73		17.30	17.31	17.00		16.38
5	H2	27.73	27.56	0.77		31.52	31.33	8.83	

*$x_0 = x_1 = x_2 = 0.04$, $y_0 = 0.9$, $y_1 = 0.04200$ and $y_2 = 0.00800$.
**$x_0 = x_1 = x_2 = 0.04$, $y_0 = 0.9$, $y_1 = 0.03975$ and $y_2 = 0.01025$.

where k represents the state of normal operation (z), and PD_{ij} is the single-sensor probability difference defined by

$$PD_{ij} = P(B_a)_{ii} - P(B_a)_{ij} \begin{cases} i = 1,\ldots,m \quad \text{and} \quad i \neq k \\ j = 1,\ldots,m, \quad j \neq i \quad \text{and} \quad j \neq k \end{cases} \quad (12)$$

Here, i denotes the state that the faulty sensor reading (R_a) is within its range, and j denotes states of node B_a other than i and k. A negative value for PI indicates false identification and the closer the value of PI is to zero, the higher is the probability of false identification. Therefore, the optimum values of the design parameters are those that maximize the IFDI performance index (PI).

Table 5 presents the values of PD_{ij} for two sets of design parameter values. Comparing the single-sensor probability difference data (which is based on one fault mode only) may result in the wrong conclusion. For example, design set 2 performs better for fault mode L2 ($8.56 > 0.48$), while set 1 shows a better performance for fault mode L1 ($17.13 > 16.22$). However, the values of the IFDI performance index imply that set 2 with a PI = 8.56 corresponds to better IFDI performance than set 1 with PI = 0.48.

Search Constraints for Optimum Values of Design Parameters. After specifying the network structure (set of nodes and directed links) in a single-sensor BBN, one needs to choose the design parameters (that is, number of states, the bin-size assignment, and prior probability data). A detailed study of the effect of the design parameters of a single-sensor BBN

Table 4. Data for the IFDI Case Study Using Model III

		Updated state Probabilities for Nodes B_a (out of 100)					Probability Absolute Difference (PAD_{ij})							
		1	2	3	4	5	1	2	3	4	5			Sensor
i	j	$n2$	$n1$	z	$p1$	$p2$	$n2$	$n1$	z	$p1$	$p2$	S_{PAD_i}	D_i	Status
							Case 1							
1	F_w	99.784	0.070	0.146	0.000	0.000	**99.784**	0.369	98.866	0.549	0.000	199.567	99.816	F^*
2	T	0.011	0.417	98.994	0.578	0.000	0.011	0.051	0.06	0.002	0.000	0.123	0.062	O^*
3	T_j	0.011	0.423	98.960	0.606	0.000	0.011	0.052	0.061	0.002	0.000	0.126	0.063	O
4	C_m	0.000	0.444	98.948	0.598	0.011	0.000	0.001	0.058	0.049	0.011	0.119	0.060	O
							Case 2							
1	F_w	4.464	21.895	73.605	0.035	0.000	4.464	**21.456**	25.407	0.514	0.000	51.842	49.777	F
2	T	0.001	0.039	74.020	20.578	5.363	0.001	0.327	25.034	**19.998**	5.363	50.724	48.704	F
3	T_j	0.070	0.707	98.625	0.598	0.000	0.070	0.336	0.396	0.010	0.000	0.811	0.779	O
4	C_m	0.000	0.438	98.628	0.867	0.068	0.000	0.007	0.378	0.318	0.068	0.771	0.740	O

F = faulty, O = operative.

on the IFDI performance of the model is needed to deduce the search constraints for optimum values of design parameters. The conditional probability data of node R_a of Model III depends on the number of states and the bin-size assignment of nodes X_a, B_a, and R_a. One can choose a different number of states for each node (Case I) or the same number of states for all nodes (Case II). We propose using the same number of states for all nodes. The conditional probability data of node R_a is closer to the ideal situation (one-to-one mapping between causes and effects) in Case II than in Case I. As a result, Case II allows one to perform fault identification more effectively. Note that Case II does not impose any limitations on the status of Model-III nodes. Furthermore, the use of Case II does not affect adversely the IFDI performance or limit the applicability of Model III.

The bin-size assignment of nodes X_a, B_a, and R_a also affects the conditional probability data of node R_a and, thus, the IFDI performance of Model III. Since node R_a is the true representation of node X_a for an operative sensor, the bin size of states of node R_a should be the same as that of the corresponding states of node X_a. Furthermore, according to Model III, any deviation from normal sensor reading for an operative sensor is due to the presence of a bias described by Eq. 1. Equation 1 implies that the size of the states of node B_a should also be the same as that of the corresponding states of node X_a. As an example, consider the parameter/variable "a" to be represented by a single-sensor BBN consisting of five-state nodes with the same states, as described earlier. On a dimensionless basis, let the bin-range assignment of state H1 of node X_a be (1.1 1.3] and the parameter/variable a be in its ideal status (1.0). For these conditions, the bin-range of state p1 of node B_a that causes the sensor reading (R_a) to shift from state N to state H1 is (0.1 0.3]. Thus, the bin sizes of states H1 and p1 are both 0.2.

The bin-size assignment of nodes X_a, B_a, and R_a has another feature that can be explained by using a property of the noise (fault type). Earlier, it was stated that Model III is capable of identifying noise, as well as other types of sensor faults. An important property of the noise is that the distribution of the senor reading is usually Gaussian. Therefore, the bin-size assignment of node B_a should be symmetric around the state z; otherwise, effective identification of the noise is not possible. This discussion on the number of states and the bin-size assignment of nodes X_a, B_a and R_a can be summarized in three rules (search constraints):

(1) The number of states of nodes X_a, B_a, and R_a should be equal.

(2) The bin size of corresponding states of nodes X_a, B_a, and R_a should be equal.

(3) The bin-size assignment of node B_a should be symmetric around the state z. Thus, the number of states of node B_a should be odd.

These rules for the five-state nodes X_a, B_a, and R_a (in a format that facilitates further discussion) are given in Table 6. The notations are defined in the Notation section.

More search constraints can be deduced on the basis of the values that x_0, x_1, and x_2 can take. When the measurement is normalized with respect to its steady-state value, under operative noise-free sensor conditions, the steady-state value and bias of the measurement are 1 and 0, respectively. Thus, the lower and upper limits for the bin ranges of states

Table 6. State Sizes for Nodes X_a, R_a and B_a

	States				
	$L2$ and $n2$	$L1$ and $n1$	N and z	$H1$ and $p2$	$H2$ and $p2$
Size	x_2	x_1	x_0	x_1	x_2

N and z are $(1.0 \pm \alpha)$ and $(0.0 \pm \alpha)$, respectively, where α is the deviation from the steady-state value of the measurement that can be tolerated in the process. The value of α depends on the process safety, control, and economic importance of the parameter/variable. For example, the allowable deviation in the steady-state value of temperature in a polymerization reactor may be 7% and 3% for low-grade and high-grade polymers, respectively. It is reasonable to assume that a reliable expert opinion on the value of α is always available. Therefore

$$x_0 = 2\alpha \tag{13}$$

For a properly-selected sensor, the value of α is also related to the sensor accuracy (β) [as a fraction of the sensor measurement]

$$\alpha \geq \beta \tag{14}$$

The bin-size assignment of node B_a affects the time required for detecting changes in the status of MPS and, hence, the fault identification performance of Model III. To show the dependency of the fault identification performance of Model III on the bin-size assignment of node B_a, two cases (a and b) of bin-size assignment for node B_a are presented in Figure 7. The size of state z for both Cases a and b are the same, because the value of α is assumed to be known. The only difference between Case a and b is that the size of states p1 and p2 (x1 and x2) in Case a is bigger than x_1 and x_2 in Case b. Figure 7 clearly shows that $\Delta t_a > \Delta t_b$, where Δt_a and Δt_b are the times needed to detect a change in the status of MPS from state z to state p2 in Cases a and b, respec-

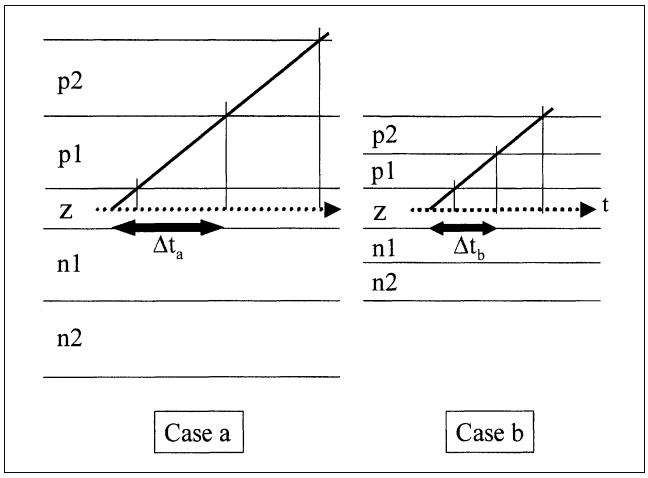

Figure 7. Effect of bin size on fault identification performance of Model III.

tively. Obviously, the smaller are x_1 and x_2, the shorter is the time needed to detect a change in the status of MPS and the better is the fault identification performance of Model III. The accuracy of the sensor limits the values that can be chosen for x_1 and x_2

$$x_1, x_2 \leq x_0, \text{ when } \alpha = \beta \tag{15}$$

Equation 15 is the fourth and the last search constraint concerning the bin-size assignment of nodes X_a, B_a, and R_a. More search constraints can be obtained by studying prior probability data of the parent nodes (X_a and B_a). For an operative sensor, node R_a cannot be the true representative of node X_a, when there is an inconsistency between the prior probability data of nodes X_a and B_a. Therefore, the prior probability distributions for nodes X_a and B_a should be the same, which is a search constraint (fifth). Another search constraint (sixth) arises from the facts that:

- The state N of node X_a and the state z of node B_a have the highest prior probability under normal operation (normal process operation and operative sensor).
- The state prior probabilities of nodes X_a and B_a (except for N and z) should decrease with the deviation of these states from states N and z.

The fact that prior probability data of node B_a is symmetrical around the state z leads to the seventh search constraint. The mutual exclusiveness of all states of nodes X_a and B_a gives rise to another search constraint (eighth). In a format that facilitates this discussion further, Table 7 presents the fifth and seventh search constraints for a five-state single-sensor BBN. The notations are defined in the Notation section. Using the notations, the sixth and eighth search constraints take the forms

Table 7. Prior Probabilities for Nodes X_a and B_a

	States				
	$L2$ and $n2$	$L1$ and $n1$	N and z	$H1$ and $p2$	$H2$ and p2
Probability	y_2	y_1	y_0	y_1	y_2

$$y_0 > y_1 > y_2 \tag{16}$$

$$y_0 + 2(y_1 + y_2) = 100 \tag{17}$$

Search constraints lower considerably the dimension of the design parameter space of a single-sensor BBN. For example, in the case of five-state nodes, the number of independent design parameters is reduced from 25 (15 design parameters for state bin size and 10 design parameters for prior probability data) to 5 (x_1, x_2, y_0, y_1, and y_2). Furthermore, the values of x_1, x_2, y_0, y_1, and y_2 are subjected to the constraints of Eqs. 15 to 17. According to the discussion presented in this subsection, one can conclude that the number of independent design parameters for a single-sensor BBN is equal to the number of the states assigned to the nodes of the BBN. Apart from the search constraints discussed in this subsection, an index is required to compare the IFDI performance of different sets of design parameter values. Such an index allows one to find the optimum value of the design parameters.

Optimum Values of Design Parameters of Model III. For a single-sensor model with m-state nodes X_a, B_a, and R_a, the optimum values of the m design parameters maximize the IFDI performance index of Eq. 11. The optimum parameter values for three cases with $\alpha = \beta = 0.02$ and m = 5, 7 and 9 are given below:

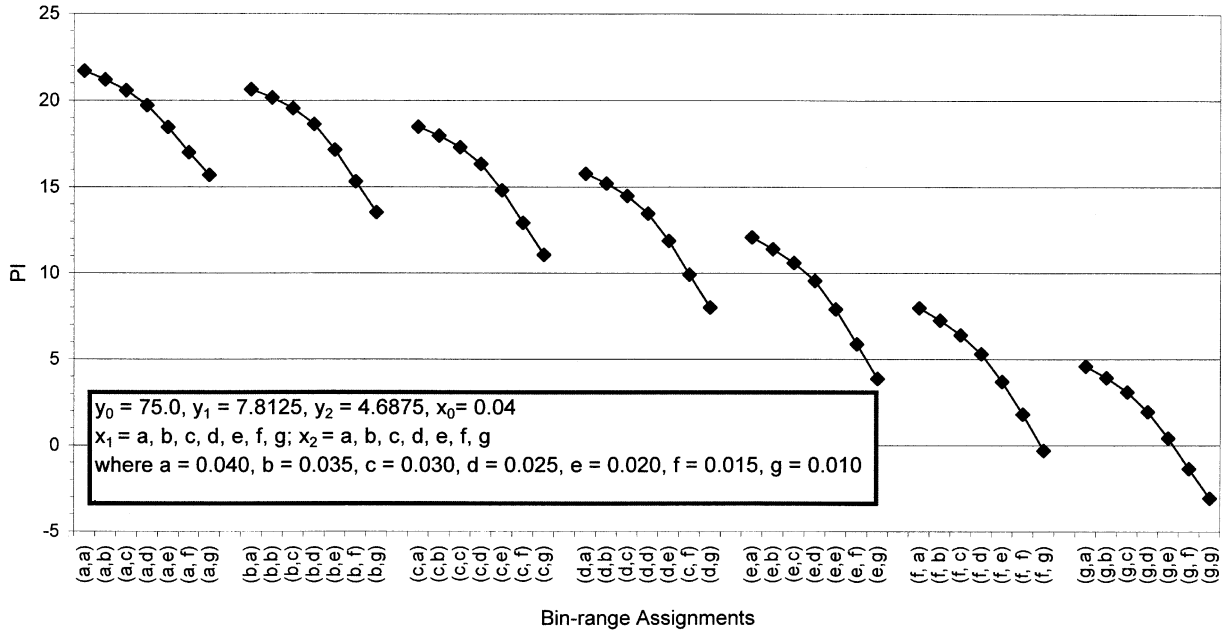

Figure 8. Effect of bin sizes on the IFDI performance index of a single-sensor BBN when prior probabilities are constant.

(1) When the prior probabilities (y_0, y_1, y_2,...) are constant, the IFDI performance index increases as the bin sizes (x_1, x_2,...) increase. This trend is shown in Figure 8 for the case with $m = 5$ and $x_0 = 2\alpha = 0.04$. This fact and the constraint of Eq. 15 leads to the conclusion that the best IFDI performance is achievable when the bin sizes of all states are equal to x_0.

(2) For the cases in which the bin sizes of all states are equal to x_0, the prior probabilities that maximize the IFDI performance index are:

(a) $m = 5$: $y_0 = 75.0, y_1 = 7.88, y_2 = 4.62$

(b) $m = 7$: $y_0 = 75.0, y_1 = 6.33, y_2 = 3.88, y_3 = 2.29$

(c) $m = 9$: $y_0 = 74.0, y_1 = 5.87, y_2 = 3.52, y_3 = 2.21, y_4 = 1.40$

The prior probability assignment (4, d) that maximizes the performance index is shown in Figure 9 for the case of five-state nodes with $x_0 = x_1 = x_2 = 0.04$. These were obtained by a systematic search among all possible values for prior probabilities subject to the constraints of Eqs. 16 and 17.

Procedure for IFDI

Maintaining essential variables of a continuous process within acceptable ranges ensures a satisfactory operation of the process at steady state. To achieve an effective IFDI, the acceptable range of every essential variable should be considered in bin-size assignment of a BBN model. In view of this and the results on the optimum design parameters and threshold setting, the following procedure for IFDI by Model III is proposed:

(1) Determine the steady-state values and the acceptable range of the essential variables (those that should be monitored and/or controlled to ensure a satisfactory operation).

(2) For each essential variable, determine the bin range of the state $N(x_0 = 2\alpha)$ of node X_a on the basis of the acceptable range of the essential variable. Different bin ranges may be assigned for different essential variables.

(3) Select a value for the number of states (m) such that the total range of interest can be covered for each essential variable. This value should be the same for all essential variables. The upper and lower limits of the total range for each essential variable can be determined from

$$\textit{Upper and lower limits} = \textit{Steady state value} \pm (m\alpha) \quad (18)$$

(4) Determine the upper and lower limits of other parameters/variables by using (i) a mathematical model of the process or process data (if available), and (ii) the upper and lower limits of the essential variables.

(5) Divide the total range (from step 4) by the number of states (m, from step 3) to get the state bin size (x_0) for process variables other than essential variables. Note that for a properly selected sensor

$$\alpha_i \geq \beta_i \quad \text{and} \quad \alpha_i = \frac{x_{0_i}}{2} \; i = 1,\ldots,n \quad (19)$$

where n is the number of measurable variables (sensors required in a multisensor BBN). Any sensor that does not meet the requirement of Eq. 19, may cause a false alarm.

(6) Use the bin-size assignment (from the previous steps) in a Monte Carlo simulation to calculate the necessary conditional probability data for single-sensor networks.

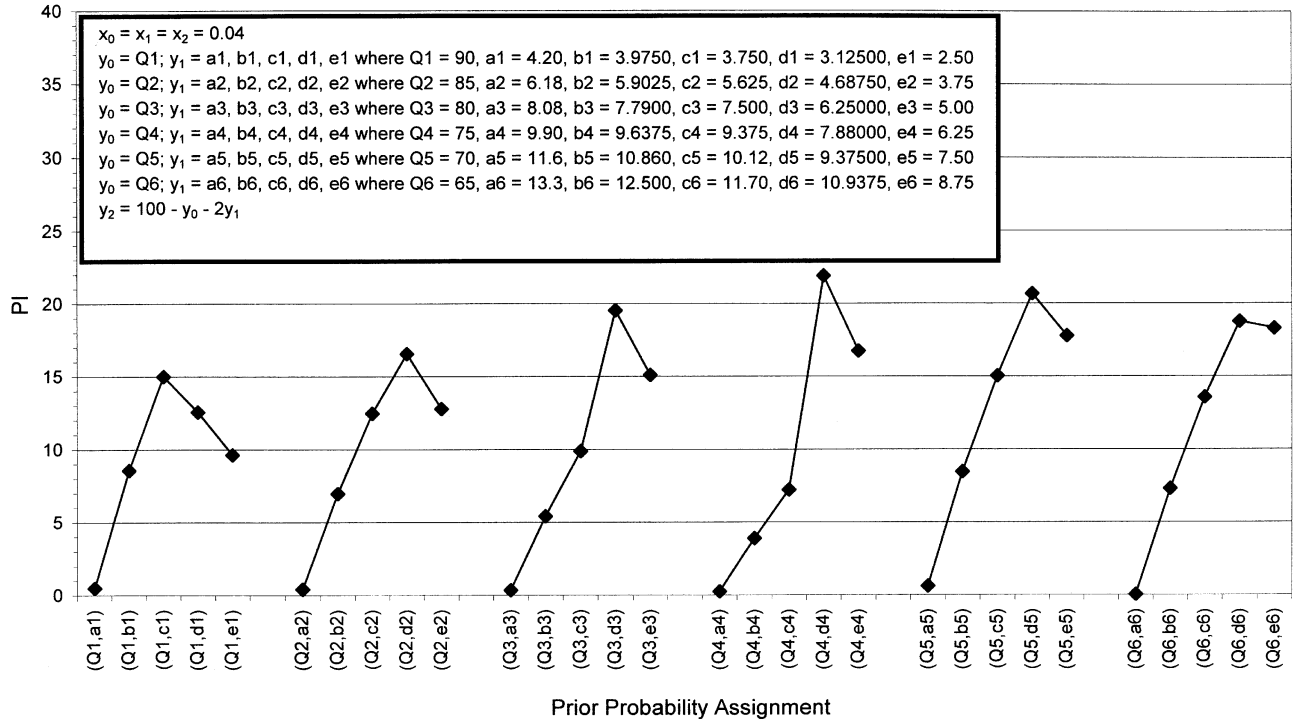

Figure 9. Effect of prior probabilities on the IFDI performance index of a single-sensor BBN when bin sizes are constant.

(7) Determine the directed links between X_a nodes of single-sensor networks by considering the process inputs as parent nodes and other variables as child nodes.

(8) Use a mathematical model of the process or fault-free process data to describe the correlation between each parent-child pair of X_a nodes of the multisensor BBN in the form of conditional probability data.

(8a) In the case of using a mathematical model of the process, a Monte Carlo simulation should be carried out to determine the conditional probability data. In the simulation, uniformly distributed random values are selected within the range of states for any combination of essential variables states. Substitution of randomly selected values of essential variables in the mathematical model allows one to determine values of other parameters/variables. The bin-size assignments calculated by applying the first five steps of the IFDI procedure are then used to map the selected random values of essential variables and the calculated values of other parameters/variables to the state space of X_a nodes. The conditional probability data between X_a nodes is determined from the probability distribution of mapped data.

(8b) In the case of using process data, the learning capabilities of Bayesian belief networks can be exploited to determine the conditional probability data. The bin-size assignments calculated by applying the first five steps should be used to map the process data representing R_a nodes to the state space of corresponding X_a nodes. The conditional probability data between each pair of X_a nodes is calculated by using the mapped process data and the directed links determined in step 7.

(9) Use the prior probability data given in the subsection on optimum values of design parameters of Model III for all parent nodes.

(10) Develop a multisensor BBN model. Determine the minimum value of the fault detection index for faulty sensors $Df_{\min}$, and the maximum value of the fault detection index for operative sensors $Do_{\max}$, by using the BBN model.

(11) Set the fault detection threshold (T_d) according to Eq. 8.

Illustrative Example

The procedure proposed in the previous subsection is applied to the polymerization reactor described in two subsections earlier. The outlet monomer concentration (C_m) has a steady-state value of 0.22967 (kmol·m^{-3}) and $\alpha = 0.022$ is considered as an essential variable. Bin-size assignments set for the measured variables of the process (according to the first five steps of the procedure for $m = 5$) are given in Table 8. According to Step 5, $\alpha = 0.0056$, 0.0092, and 0.0798 for T, T_j, and F_w, respectively, assuming that $\alpha > \beta$ holds for all sensors. The steady-state version of the mathematical model of the polymerization reactor is used to calculate the conditional probabilities needed to build a multisensor BBN model for the process sensors. The multisensor BBN model is shown in Figure 6. $Df_{\min}$ and $Do_{\max}$ are then calculated according to Step 10 ($Df_{\min} = 16.5$ and $Do_{\max} = 8.9$). Since no preference between missed faults and false alarms is assumed, the midway between 16.5 and 8.9 (that is, 12.7) is considered as the value of the fault detection threshold (T_d). Three cases are considered to study the performance of the developed BBN-based IFDI method. Case I deals with three different single faults (of types: bias, drift and noise). Cases II and III consider two simultaneous faults. The bin-size assignments given in Table 8 are used to map the simulated data for operative and faulty sensors to the state space of R_a nodes. The mapped sensor data at each sampling instance are introduced to the multisensor BBN of Figure 6 as evidence. Inference process updates the probability distribution of X_a nodes that are used to calculate the fault detection index and MPS for sensors of the reactor. To present the results of fault detection and identification, a fault flag is used. The value of the fault flag represents the fault type. A fault flag of 0 represents an operative sensor, while 1, 2, and 3 represent noise, bias and drift, respectively. The fault identification criteria that were considered are:

- A constant MPS over 10 sampling periods or more is considered as bias.
- A steady fluctuation of MPS between different states of bias for more than 3 sampling periods is considered as noise.
- A constant MPS less than 10 sampling periods followed by MPS in a higher or lower state of bias (steady gradual change of MPS) is considered as drift.
- Any incipient sensor fault is considered as noise till correct identification is feasible.

Case I: single fault

The single faults are introduced to the sensor reading of the cooling water flow rate (F_w) over 120 sampling periods. During this time interval, other sensors are assumed to be operative (sensor readings are within the range of state N). Figure 10 shows dimensionless sensor reading (sensor reading divided by its steady-state value), fault detection index for the four sensors, the status of MPS for the faulty sensor, and the fault flag. The maximum value of the fault detection in-

Table 8. Bin-Range Assignment* for Nodes X_a and R_a for the Illustrative Example

		States									
		$L2$		$L1$		N		$H1$		$H2$	
a	Factor	ll**	ul**	ll	ul	ll	ul	ll	ul	ll	ul
F_w	10^{-3}	[4.022	5.089)	[5.089	6.156)	[6.156	7.223]	(7.223	8.289]	(8.289	9.356]
T	10^{2}	[4.517	4.548)	[4.548	4.580)	[4.580	4.612]	(4.612	4.643]	(4.643	4.676]
T_j	10^{2}	[4.332	4.382)	[4.382	4.432)	[4.432	4.481]	(4.481	4.531]	(4.531	4.581]
C_m	10^{-2}	[20.467	21.467)	[21.467	22.467)	[22.467	23.467]	(23.467	24.467]	(24.467	25.467]

*The steady states and dimensions are the same as those shown in Table 1.
**ll = lower limit; ul = upper limit.

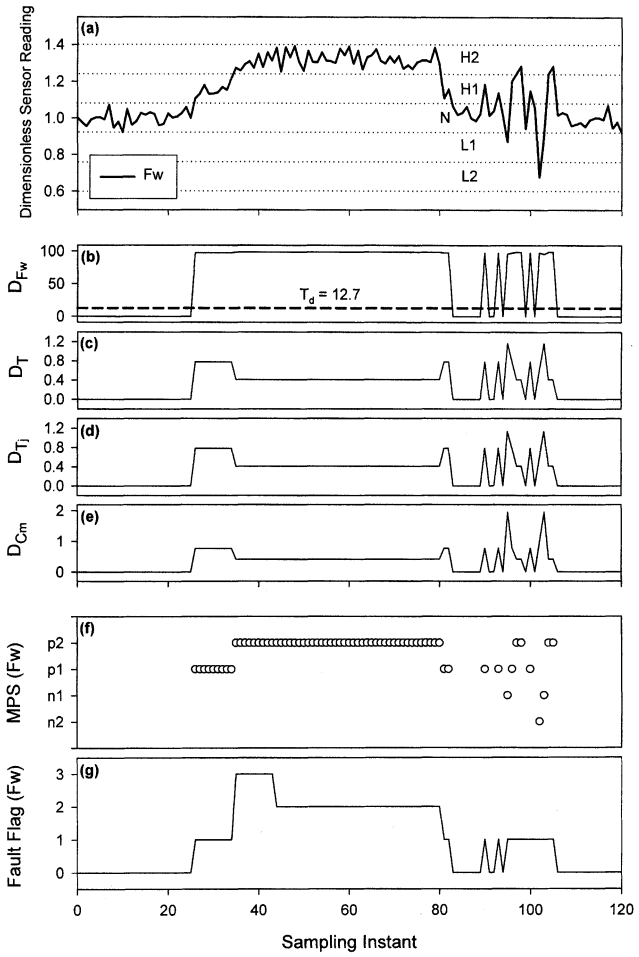

Figure 10. IFDI when a single fault (drift, bias or noise) is present: Case I.

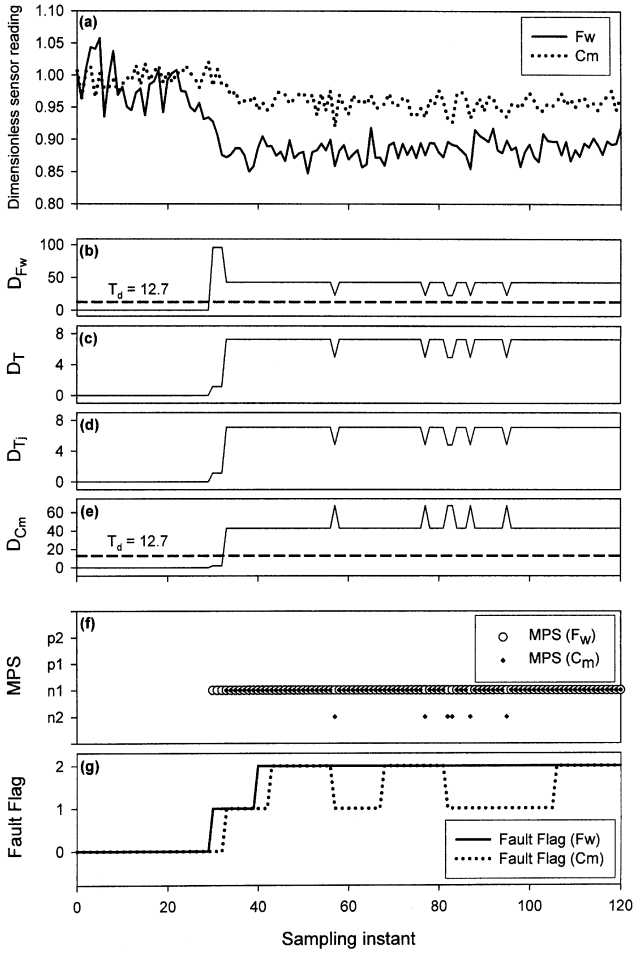

Figure 11. IFDI when two simultaneous bias faults are present: Case II.

dex for the T, T_j, and C_m sensors (operative sensors) is 1.95. The minimum value of the fault detection index for the F_w sensor (faulty sensor) is 95.75 when the fault is present. The assigned value for fault detection threshold (12.7), and the considerable difference between 1.95 and 95.75 allow effective fault detection without delay. Table 9 presents the start and end time instants for each fault type and the time instant of each correct identification. The effect of the fault identification criteria (listed in the previous subsection) on identification time delay is clearly reflected in the data presented in Table 9. As can be seen, there is no identification time delay for the noise fault, and the maximum identification time delay is for the drift fault (9 sampling periods). There are two normal sensor readings during the occurrence of the noise fault. These normal sensor readings cause the identification time delay for the noise fault to be five sampling instants.

Table 9. Starting Time Instant of Faults and Fault Identification Time Instant in Case I of the Illustrative Example

	Fault Type		
Time Instant	Drift	Bias	Noise
Start	26	39	90
Identification	35	44	95

Case II: multiple faults

A case of two ($l = 2$) simultaneous bias faults in the cooling-water-flow-rate and outlet-monomer-concentration sensors is considered to evaluate the performance of the IFDI method when multiple faults occur. Figure 11 presents dimensionless sensor readings, fault detection indices for different sensors, MPS, and fault flags for the faulty sensors. The maximum value of fault detection index for the sensors measuring T and T_j (operative sensors) is 7.29. The minimum value of the fault detection index for the sensors that measures F_w and C_m (faulty sensors) is 22.71 when the faults are present. Despite a considerable decrease in the difference between the maximum and minimum values of fault detection index for operative and faulty sensors, effective IFDI is still feasible. The two simultaneous faults do not emerge at the same sampling instant and, as shown in plot (g) of Figure 11, the IFDI method successfully captures the difference in fault starting times. The wrong switching of fault flag for outlet monomer concentration from 2 to 1 at sampling instants 57 and 81 is due to a change in MPS from state n1 to state n2 for one or two sampling periods. The delay to switch back to correct identification at sampling instances 68 and 106 is due to the fault identification criterion for bias.

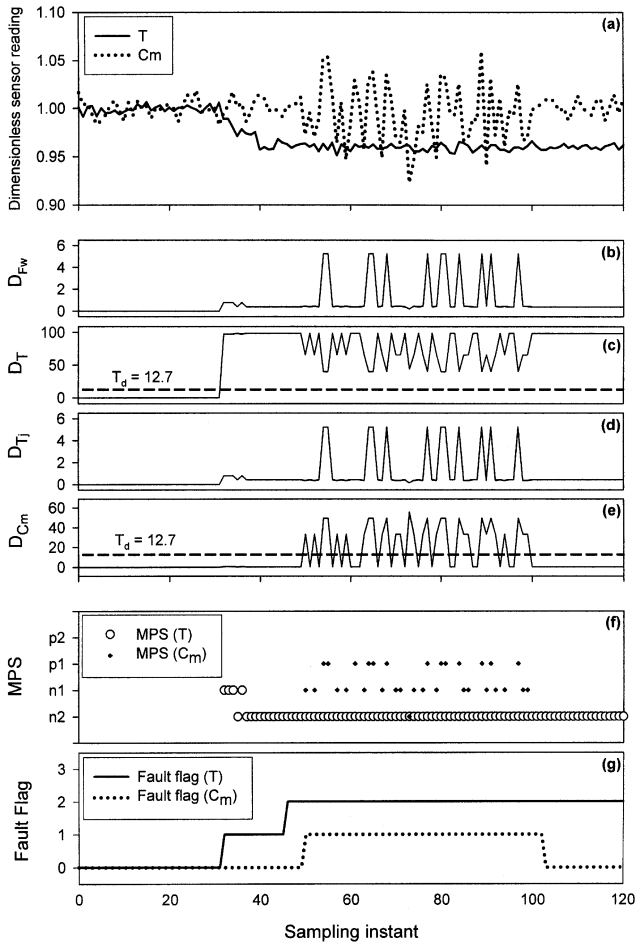

Figure 12. IFDI when two simultaneous bias and precision-degradation faults are present: Case III.

Case III: multiple faults

Another case of two ($l = 2$) simultaneous faults in the reactor-temperature and outlet-monomer-concentration sensors is also presented here to show the capabilities of the developed IFDI method in detecting and identifying multiple faults of different types. The fault types are bias and noise for the sensors. The result of IFDI for this case is presented in Figure 12. The maximum value of the fault detection index for the T_j and F_w sensors (that are operative sensors) is 5.26. The minimum value of fault detection index for the sensors that measures T and C_m (faulty sensors) is 33.40 when the faults are present. The difference between the maximum and minimum value of fault detection index for operative and faulty sensors and the value of fault detection threshold (12.7) allow effective IFDI. As can be seen in Figure 12, the dissimilarity of fault types is not a limitation for an effective IFDI by the method.

Conclusions

A single-sensor BBN model was proposed. In contrast to the existing models, it has the capabilities needed to carry out a complete IFDI. The IFDI performance of the model was studied, and the optimum values of the design parameters that make effective fault detection and identification possible were given. A multisensor, BBN-based IFDI method was developed. The necessity of a new approach of threshold setting for the developed IFDI method was discussed, and such an approach was presented. Guidelines were presented to facilitate the application of the developed method, and the illustrative examples were given to show the performance of the method. The examples showed that the method is capable of detecting single and multiple sensor faults, and identifying the three fault types (bias, drift, and noise). While capable of identifying the three fault types, the developed method cannot identify sensor complete failure.

The application of BBN in IFDI presented here revealed some potentials of BBN. More studies are needed to explore other potentials of BBN. Future work includes extending the method to transient processes, and investigating the possibility of performing process fault detection and diagnosis along with IFDI. Frequency of fault types I and II is a good measure of the efficiency of an IFDI method. Future work also includes conducting simulations and applying this BBN-based and the other IFDI methods (such as those that are based on PCA and Kalman filtering) to industrial processes to determine relative advantages and disadvantages of the IFDI methods.

Notation

A = un-instantiated prepositional variable
a = parameter/variable that is measured
B_a = node representing the bias associated with X_a
C_{ii} = concentration of initiator in the initiator inlet stream ($kmol \cdot m^{-3}$)
C_m = concentration of monomer in the outlet stream ($kmol \cdot m^{-3}$)
C_{mm} = concentration of monomer in the monomer inlet stream ($kmol \cdot m^{-3}$)
CP = conditional probability distribution of child nodes in a BBN
Df_{min} = minimum of fault detection indices of faulty sensors
D_i = fault detection index of sensor i
Do_{max} = maximum of fault detection indices of operative sensors
E = instantiated prepositional variable (evidence)
F_w = cooling water flow rate ($m^3 \cdot s^{-1}$)
H1 = state of nodes R_a and X_a representing the actual value of the parameter/variable a and the available measurement in the range of high
H2 = state of nodes R_a and X_a representing the actual value of the parameter/variable a and the available measurement in the range of very high
I_i = fault identification index of sensor i
L = set of directed links in a BBN
l = number of simultaneously-faulty sensors in a multisensor BBN
L1 = state of nodes R_a and X_a representing the actual value of the parameter/variable a and the available measurement in the range of low
L2 = state of nodes R_a and X_a representing the actual value of the parameter/variable a and the available measurement in the range of very low
m = number of states for each node in a multisensor BBN
MPS = most probable state (state of node B_a that is most probably responsible for the detected fault)
n = number of sensors in a multisensor BBN

N = state of nodes R_a and X_a representing normal condition for actual value of the parameter/variable a and available measurement
$n_{1/2}$ = half number
$n1$ = state of node B_a representing bias in the range of negative
$n2$ = state of node B_a representing bias in the range of very negative
N_a = node representing the noise associated with X_a
P = state probability of a prepositional variable
P^* = state probability of a prepositional variable in operative mode
$p1$ = state of node B_a representing bias in the range of positive
$p2$ = state of node B_a representing bias in the range of very positive
PAD_{ij} = probability absolute difference of state j of sensor i
PP = prior probability distribution of parent nodes in a BBN
R_a = node representing the available measurement for X_a
S_{PAD_i} = sum of probability absolute differences of sensor i
T = reactor temperature, K
T_d = fault detection threshold
T_j = jacket temperature, K
V = set of variables or nodes in a BBN
x_0 = bin size of the state N of nodes R_a and X_a, and state z of node B_a
x_1 = bin size of the states L1 and H1 of nodes R_a and X_a, and states n1 and p1 of node B_a
x_2 = bin size of the states L2 and H2 of nodes R_a and X_a, and states n2 and p2 of node B_a
X_a = node representing the actual value of the parameter/variable a
y_0 = prior probability of state N of node X_a, and state z of node B_a
y_1 = prior probability of state L1 of node X_a, and state n1 of node B_a
y_2 = prior probability of state L2 of node X_a, and state n2 of node B_a
z = state of node B_a representing zero bias

Greek letters

α = acceptable deviation of a parameter/variable from its steady-state value
β = sensor accuracy (fraction of the sensor reading)
Δt_a = time needed to detect a change in the status of MPS for Case a of Figure 7
Δt_b = time needed to detect a change in the status of MPS for Case b of Figure 7
σ = standard deviation of a sensor reading sample

Literature Cited

Alag, S., K. Goebel, and A. Agogino, "A Methodology for Intelligent Sensor Validation and Fusion used in Tracking and Avoidance of Objects for Automated Vehicles," *Proc. of Amer. Contr. Conf.*, Seattle, WA, 3647 (1995).

Aldrich, C., and J. S. J. Van Deventer, "Identification of Gross Errors in Material Balance Measurements by Means of Neural Nets," *Chem. Eng. Sci.*, **49**, 1357 (1994).

Aradhye, H. B., "Sensor Fault Detection, Isolation, and Accommodation Using Neural Networks, Fuzzy Logic, and Bayesian Belief Networks," M.S. Diss., University of New Mexico, Albuquerque, NM (1997).

Betta, G., and A. Pietrosanto, "Instrument Fault Detection and Isolation: State of the Art and New Research Trends," *IEEE Trans. Instr. and Meas.*, **49**, 100 (2000).

Bulsari, A., A. Medvedev, and H. Saxen, "Sensor Fault Detection Using State Vector Estimator and Feed-Forward Neural Networks Applied to a Simulated Biochemical Process," *Acta Polytech. Scand., Chem. Technol. Metall. Ser.*, **20**, 199 (1991).

Clark, R. N., "Instrument fault detection," *IEEE Trans. Aerosp. Electron. Syst.*, **14**, 456 (1978a).

Clark, R. N., "A Simplified Instrument Failure Detection Scheme," *IEEE Trans. Aerosp. Electron. Syst.*, **14**, 558 (1978b).

Clark, R. N., D. C. Fosth, and V. M. Walton, "Detection Instrument Malfunction in Control Systems," *IEEE Trans. Aerosp. Electron. Syst.*, **11**, 465 (1975).

Dorr, R., F. Kratz, J. Ragot, F. Loisy, and J. L. Germain, "Detection, Isolation, and Identification of Sensor Faults in Nuclear Power Plants," *IEEE Trans. Contr. Syst. Techn.*, **5**, 42 (1997).

Dunia, R., S. J. Qin, T. F. Edgar and T. J. McAvoy, "Identification of Faulty Sensors Using Principal Component Analysis," *AIChE J.*, **42**, 2797 (1996).

Frank, P. M., and L. Keller, "Sensitivity Discriminating Observer Design for Instrument Failure Detection," *IEEE Trans. Aerosp. Electron. Syst.*, **16**, 456 (1980).

Gertler, J. J., and T. J. McAvoy, "Principal Component Analysis and Parity Relations-A Strong Duality," *IFAC SAFEPROCESS Symp.*, **2**, 837 (1997).

Gertler, J. J., W. Li, Y. Huang, and T. J. McAvoy, "Isolation Enhanced Principal Component Analysis," *AIChE J.*, **29**, 243 (1999).

Gupta, G., and N. Shankar, "Application of Neural Networks for Gross Error Detection," *Ind. Eng. Chem. Res.*, **32**, 1651 (1993).

Hidalgo, P. M., and C. B. Brosilow, "Nonlinear Model Predictive Control of Styrene Polymerization at Unstable Operating Points," *Comput. Chem. Eng.*, **14**, 481 (1990).

Ibarguengoytia, P. H., L. E. Sucar, and S. Vadera, "A Probabilistic Model for Sensor Validation," *Proc. Conf. on Uncertainty in Artificial Intelligence*, Portland, OR, 332 (1996).

Kirch, H., and K. Kroschel, "Applying Bayesian Networks to Fault Diagnosis," *Proc. of IEEE Conf. on Control Applications*, 895 (1994).

Kramer, M. A., "Autoassociative Neural Networks," *Comput. Chem. Eng.*, **16**, 313 (1992).

Kresta, J. V., J. F. MacGregor, and T. E. Marlin, "Multivariate Statistical Monitoring of Processes," *Can. J. Chem. Eng.*, **69** 35 (1991).

Lauritzen, S. L., and D. J. Spieglhalter, "Local Computation with Probabilities on Graphical Structures and Their Application to Expert Systems," *J. Roy. Stat. Soc.*, B, **50**, 157 (1988).

Lee, W. Y., J. M. House, and D. R. Shin, "Fault Diagnosis and Temperature Sensor Recovery for an Air-Handling Unit," *ASHRAE Trans.*, **103** 621 (1997).

MacGregor, J. F., "Multivariate Statistical Methods for Monitoring Large Databases from Chemical Processes," AIChE Meeting, San Francisco (1989).

Mehra, R. K., and I. Peshon, "An Innovations Approach to Fault Detection and Diagnosis in Dynamic Systems," *Automatica*, **7**, 637 (1971).

Nicholson, A. E., and J. M. Brady, "Sensor Validation Using Dynamic Belief Networks," *Proc. of 8th Conf. on Uncertainty in Artifi. Intell.*, 207 (1992).

Park, S., and C. S. G. Lee, "Fusion-Based Sensor Fault Detection," *Proc. of Int. Symp. on Intelligent Contr.*, Chicago, 156 (1993).

Patton, R. J. and J. Chen, "Observer-Based Fault Detection and Isolation: Robustness and Applications," *Control Eng. Practice*, **5**, 671 (May 1997).

Piovoso, M. J., K. A. Kosanovich, and P. K. Pearson, "Monitoring Process Performance in Real Time," *Proc. Amer. Control Conf.*, Chicago, 2359 (1992a).

Piovoso, M. J., K. A. Kosanovich, and J. P. Yuk, "Process Data Chemometrica," *IEEE Trans. Instr. and Meas.*, **41**, 262 (1992b).

Qin, S. J. and W. Li, "Detection, Identification, and Reconstruction of Faulty Sensors with Maximized Sensitivity," *AIChE J.*, **45**(9), 1813 (1999).

Rojas-Guzman, C., and M. A. Kramer, "Comparison of Belief Networks and Rule-based Expert Systems for fault Diagnosis of Chemical," *Eng. Applic. Artif. Intell.*, **6**, 191 (1993).

Sanchez, M., G. Sentoni, S. Schbib, S. Tonelli, and J. Romagnoli, "Gross Measurements Error Detection/Identification for an Industrial Ethylene Reactor," *Comput. Chem. Eng.*, **20**(972), S1559 (1996).

Santoso, N. I., C. Darken, and G. Povh, "Nuclear Plant Fault Diagnosis Using Probabilistic Reasoning," *Power Eng. Soc. Summer Meeting, IEEE*, **2**, 714 (1999).

Terry, P. A., and D. M. Himmelblau, "Data Rectification and Gross Error Detection in a Steady-State Process Via Artificial Neural Networks," *Ind. Eng. Chem. Res.*, **32**, 3020 (1993).

Valle, S., J. S. Qin, and M. J. Piovoso, "Analysis of Multi-Block PCA and PLS for Fault Detection and Identification," AIChE Meeting, Los Angeles (2000).

Watanabe, K., and D. M. Himmelblau, "Instrument Fault Detection in Systems with Uncertainties," *Int. J. Syst. Sci.*, **13**, 73 (1982).
Watanabe, K., A. Komori, and T. Kiyama, "Diagnosis of Instrument Fault," *Proc. IEEE IMTC*, Hamamatsu, Japan, 386 (1994).
Wise, B. M., N. B. Gallagher, and J. F. MacGregor, "The Process Chemometrics Approach to Process Monitoring and Fault Detection," *Proc. IFAC Workshop on On-Line Fault Detection and Supervision in the Chemical Industries*, Newcastle, U.K., 1 (1995).
Yoon, S., and J. F. MacGregor, "PCA of Multiscale Data and its Application to Fault Isolation," AIChE Meeting, Los Angeles (2000).

Manuscript received June 28, 2002, and revision received Feb. 4, 2003.